

Observation of $\eta_c(1S)$ and $\eta_c(2S)$ decays to $K^+K^-\pi^+\pi^-\pi^0$ in two-photon interactions

P. del Amo Sanchez,¹ J. P. Lees,¹ V. Poireau,¹ E. Prencipe,¹ V. Tisserand,¹ J. Garra Tico,² E. Grauges,² M. Martinelli^{ab,3} A. Palano^{ab,3} M. Pappagallo^{ab,3} G. Eigen,⁴ B. Stugu,⁴ L. Sun,⁴ M. Battaglia,⁵ D. N. Brown,⁵ B. Hooberman,⁵ L. T. Kerth,⁵ Yu. G. Kolomensky,⁵ G. Lynch,⁵ I. L. Osipenkov,⁵ T. Tanabe,⁵ C. M. Hawkes,⁶ A. T. Watson,⁶ H. Koch,⁷ T. Schroeder,⁷ D. J. Asgeirsson,⁸ C. Hearty,⁸ T. S. Mattison,⁸ J. A. McKenna,⁸ A. Khan,⁹ A. Randle-Conde,⁹ V. E. Blinov,¹⁰ A. R. Buzykaev,¹⁰ V. P. Druzhinin,¹⁰ V. B. Golubev,¹⁰ A. P. Onuchin,¹⁰ S. I. Serednyakov,¹⁰ Yu. I. Skovpen,¹⁰ E. P. Solodov,¹⁰ K. Yu. Todyshev,¹⁰ A. N. Yushkov,¹⁰ M. Bondioli,¹¹ S. Curry,¹¹ D. Kirkby,¹¹ A. J. Lankford,¹¹ M. Mandelkern,¹¹ E. C. Martin,¹¹ D. P. Stoker,¹¹ H. Atmacan,¹² J. W. Gary,¹² F. Liu,¹² O. Long,¹² G. M. Vitug,¹² C. Campagnari,¹³ T. M. Hong,¹³ D. Kovalskiy,¹³ J. D. Richman,¹³ C. West,¹³ A. M. Eisner,¹⁴ C. A. Heusch,¹⁴ J. Kroseberg,¹⁴ W. S. Lockman,¹⁴ A. J. Martinez,¹⁴ T. Schalk,¹⁴ B. A. Schumm,¹⁴ A. Seiden,¹⁴ L. O. Winstrom,¹⁴ C. H. Cheng,¹⁵ D. A. Doll,¹⁵ B. Echenard,¹⁵ D. G. Hitlin,¹⁵ P. Ongmongkolkul,¹⁵ F. C. Porter,¹⁵ A. Y. Rakitin,¹⁵ R. Andreassen,¹⁶ M. S. Dubrovin,¹⁶ G. Mancinelli,¹⁶ B. T. Meadows,¹⁶ M. D. Sokoloff,¹⁶ P. C. Bloom,¹⁷ W. T. Ford,¹⁷ A. Gaz,¹⁷ M. Nagel,¹⁷ U. Nauenberg,¹⁷ J. G. Smith,¹⁷ S. R. Wagner,¹⁷ R. Ayad,^{18,*} W. H. Toki,¹⁸ H. Jasper,¹⁹ T. M. Karbach,¹⁹ J. Merkel,¹⁹ A. Petzold,¹⁹ B. Spaan,¹⁹ K. Wacker,¹⁹ M. J. Kobel,²⁰ K. R. Schubert,²⁰ R. Schwierz,²⁰ D. Bernard,²¹ M. Verderi,²¹ P. J. Clark,²² S. Playfer,²² J. E. Watson,²² M. Andreotti^{ab,23} D. Bettoni^{a,23} C. Bozzi^{a,23} R. Calabrese^{ab,23} A. Cecchi^{ab,23} G. Cibinetto^{ab,23} E. Fioravanti^{ab,23} P. Franchini^{ab,23} E. Luppi^{ab,23} M. Munerato^{ab,23} M. Negrini^{ab,23} A. Petrella^{ab,23} L. Piemontese^{a,23} R. Baldini-Ferrolì,²⁴ A. Calcaterra,²⁴ R. de Sangro,²⁴ G. Finocchiaro,²⁴ M. Nicolaci,²⁴ S. Pacetti,²⁴ P. Patteri,²⁴ I. M. Peruzzi,^{24,†} M. Piccolo,²⁴ M. Rama,²⁴ A. Zallo,²⁴ R. Contri^{ab,25} E. Guido^{ab,25} M. Lo Vetere^{ab,25} M. R. Monge^{ab,25} S. Passaggio^{a,25} C. Patrignani^{ab,25} E. Robutti^{a,25} S. Tosi^{ab,25} B. Bhuyan,²⁶ V. Prasad,²⁶ C. L. Lee,²⁷ M. Morii,²⁷ A. Adametz,²⁸ J. Marks,²⁸ U. Uwer,²⁸ F. U. Bernlochner,²⁹ M. Ebert,²⁹ H. M. Lacker,²⁹ T. Lueck,²⁹ A. Volk,²⁹ P. D. Dauncey,³⁰ M. Tibbetts,³⁰ P. K. Behera,³¹ U. Mallik,³¹ C. Chen,³² J. Cochran,³² H. B. Crawley,³² L. Dong,³² W. T. Meyer,³² S. Prell,³² E. I. Rosenberg,³² A. E. Rubin,³² A. V. Gritsan,³³ Z. J. Guo,³³ N. Arnaud,³⁴ M. Davier,³⁴ D. Derkach,³⁴ J. Firmino da Costa,³⁴ G. Grosdidier,³⁴ F. Le Diberder,³⁴ A. M. Lutz,³⁴ B. Malaescu,³⁴ A. Perez,³⁴ P. Roudeau,³⁴ M. H. Schune,³⁴ J. Serrano,³⁴ V. Sordini,^{34,‡} A. Stocchi,³⁴ L. Wang,³⁴ G. Wormser,³⁴ D. J. Lange,³⁵ D. M. Wright,³⁵ I. Bingham,³⁶ C. A. Chavez,³⁶ J. P. Coleman,³⁶ J. R. Fry,³⁶ E. Gabathuler,³⁶ R. Gamet,³⁶ D. E. Hutchcroft,³⁶ D. J. Payne,³⁶ C. Touramanis,³⁶ A. J. Bevan,³⁷ F. Di Lodovico,³⁷ R. Sacco,³⁷ M. Sigamani,³⁷ G. Cowan,³⁸ S. Paramesvaran,³⁸ A. C. Wren,³⁸ D. N. Brown,³⁹ C. L. Davis,³⁹ A. G. Denig,⁴⁰ M. Fritsch,⁴⁰ W. Gradl,⁴⁰ A. Hafner,⁴⁰ K. E. Alwyn,⁴¹ D. Bailey,⁴¹ R. J. Barlow,⁴¹ G. Jackson,⁴¹ G. D. Lafferty,⁴¹ J. Anderson,⁴² R. Cenci,⁴² A. Jawahery,⁴² D. A. Roberts,⁴² G. Simi,⁴² J. M. Tuggle,⁴² C. Dallapiccola,⁴³ E. Salvati,⁴³ R. Cowan,⁴⁴ D. Dujmic,⁴⁴ G. Sciolla,⁴⁴ M. Zhao,⁴⁴ D. Lindemann,⁴⁵ P. M. Patel,⁴⁵ S. H. Robertson,⁴⁵ M. Schram,⁴⁵ P. Biassoni^{ab,46} A. Lazzaro^{ab,46} V. Lombardo^{a,46} F. Palombo^{ab,46} S. Stracka^{ab,46} L. Cremaldi,⁴⁷ R. Godang,^{47,§} R. Kroeger,⁴⁷ P. Sonnek,⁴⁷ D. J. Summers,⁴⁷ X. Nguyen,⁴⁸ M. Simard,⁴⁸ P. Taras,⁴⁸ G. De Nardo^{ab,49} D. Monorchio^{ab,49} G. Onorato^{ab,49} C. Sciacca^{ab,49} G. Raven,⁵⁰ H. L. Snoek,⁵⁰ C. P. Jessop,⁵¹ K. J. Knoepfel,⁵¹ J. M. LoSecco,⁵¹ W. F. Wang,⁵¹ L. A. Corwin,⁵² K. Honscheid,⁵² R. Kass,⁵² J. P. Morris,⁵² N. L. Blount,⁵³ J. Brau,⁵³ R. Frey,⁵³ O. Igonkina,⁵³ J. A. Kolb,⁵³ R. Rahmat,⁵³ N. B. Sinev,⁵³ D. Strom,⁵³ J. Strube,⁵³ E. Torrence,⁵³ G. Castelli^{ab,54} E. Feltresi^{ab,54} N. Gagliardi^{ab,54} M. Margoni^{ab,54} M. Morandin^{a,54} M. Posocco^{a,54} M. Rotondo^{a,54} F. Simonetto^{ab,54} R. Stroili^{ab,54} E. Ben-Haim,⁵⁵ G. R. Bonneaud,⁵⁵ H. Briand,⁵⁵ G. Calderini,⁵⁵ J. Chauveau,⁵⁵ O. Hamon,⁵⁵ Ph. Leruste,⁵⁵ G. Marchiori,⁵⁵ J. Ocariz,⁵⁵ J. Prendki,⁵⁵ S. Sitt,⁵⁵ M. Biasini^{ab,56} E. Manoni^{ab,56} A. Rossi^{ab,56} C. Angelini^{ab,57} G. Batignani^{ab,57} S. Bettarini^{ab,57} M. Carpinelli^{ab,57,¶} G. Casarosa^{ab,57} A. Cervelli^{ab,57} F. Forti^{ab,57} M. A. Giorgi^{ab,57} A. Lusiani^{ac,57} N. Neri^{ab,57} E. Paoloni^{ab,57} G. Rizzo^{ab,57} J. J. Walsh^{a,57} D. Lopes Pegna,⁵⁸ C. Lu,⁵⁸ J. Olsen,⁵⁸ A. J. S. Smith,⁵⁸ A. V. Telnov,⁵⁸ F. Anulli^{a,59} E. Baracchini^{ab,59} G. Cavoto^{a,59} R. Faccini^{ab,59} F. Ferrarotto^{a,59} F. Ferroni^{ab,59} M. Gaspero^{ab,59} L. Li Gioi^{a,59} M. A. Mazzoni^{a,59} G. Piredda^{a,59} F. Renga^{ab,59} T. Hartmann,⁶⁰ T. Leddig,⁶⁰ H. Schröder,⁶⁰ R. Waldi,⁶⁰ T. Auye, ⁶¹ B. Franek,⁶¹ E. O. Olaiya,⁶¹ F. F. Wilson,⁶¹ S. Emery,⁶² G. Hamel de Monchenault,⁶² G. Vasseur,⁶² Ch. Yèche,⁶²

M. Zito,⁶² M. T. Allen,⁶³ D. Aston,⁶³ D. J. Bard,⁶³ R. Bartoldus,⁶³ J. F. Benitez,⁶³ C. Cartaro,⁶³ M. R. Convery,⁶³ J. Dorfan,⁶³ G. P. Dubois-Felsmann,⁶³ W. Dunwoodie,⁶³ R. C. Field,⁶³ M. Franco Sevilla,⁶³ B. G. Fulsom,⁶³ A. M. Gabareen,⁶³ M. T. Graham,⁶³ P. Grenier,⁶³ C. Hast,⁶³ W. R. Innes,⁶³ M. H. Kelsey,⁶³ H. Kim,⁶³ P. Kim,⁶³ M. L. Kocian,⁶³ D. W. G. S. Leith,⁶³ S. Li,⁶³ B. Lindquist,⁶³ S. Luitz,⁶³ V. Luth,⁶³ H. L. Lynch,⁶³ D. B. MacFarlane,⁶³ H. Marsiske,⁶³ D. R. Muller,⁶³ H. Neal,⁶³ S. Nelson,⁶³ C. P. O'Grady,⁶³ I. Ofte,⁶³ M. Perl,⁶³ T. Pulliam,⁶³ B. N. Ratcliff,⁶³ A. Roodman,⁶³ A. A. Salnikov,⁶³ V. Santoro,⁶³ R. H. Schindler,⁶³ J. Schwiening,⁶³ A. Snyder,⁶³ D. Su,⁶³ M. K. Sullivan,⁶³ S. Sun,⁶³ K. Suzuki,⁶³ J. M. Thompson,⁶³ J. Va'vra,⁶³ A. P. Wagner,⁶³ M. Weaver,⁶³ C. A. West,⁶³ W. J. Wisniewski,⁶³ M. Wittgen,⁶³ D. H. Wright,⁶³ H. W. Wulsin,⁶³ A. K. Yarritu,⁶³ C. C. Young,⁶³ V. Ziegler,⁶³ X. R. Chen,⁶⁴ W. Park,⁶⁴ M. V. Purohit,⁶⁴ R. M. White,⁶⁴ J. R. Wilson,⁶⁴ S. J. Sekula,⁶⁵ M. Bellis,⁶⁶ P. R. Burchat,⁶⁶ A. J. Edwards,⁶⁶ T. S. Miyashita,⁶⁶ S. Ahmed,⁶⁷ M. S. Alam,⁶⁷ J. A. Ernst,⁶⁷ B. Pan,⁶⁷ M. A. Saeed,⁶⁷ S. B. Zain,⁶⁷ N. Guttman,⁶⁸ A. Soffer,⁶⁸ P. Lund,⁶⁹ S. M. Spanier,⁶⁹ R. Eckmann,⁷⁰ J. L. Ritchie,⁷⁰ A. M. Ruland,⁷⁰ C. J. Schilling,⁷⁰ R. F. Schwitters,⁷⁰ B. C. Wray,⁷⁰ J. M. Izen,⁷¹ X. C. Lou,⁷¹ F. Bianchi^{ab},⁷² D. Gamba^{ab},⁷² M. Pelliccioni^{ab},⁷² M. Bomben^{ab},⁷³ L. Lanceri^{ab},⁷³ L. Vitale^{ab},⁷³ N. Lopez-March,⁷⁴ F. Martinez-Vidal,⁷⁴ D. A. Milanes,⁷⁴ A. Oyanguren,⁷⁴ J. Albert,⁷⁵ Sw. Banerjee,⁷⁵ H. H. F. Choi,⁷⁵ K. Hamano,⁷⁵ G. J. King,⁷⁵ R. Kowalewski,⁷⁵ M. J. Lewczuk,⁷⁵ I. M. Nugent,⁷⁵ J. M. Roney,⁷⁵ R. J. Sobie,⁷⁵ T. J. Gershon,⁷⁶ P. F. Harrison,⁷⁶ T. E. Latham,⁷⁶ E. M. T. Puccio,⁷⁶ H. R. Band,⁷⁷ S. Dasu,⁷⁷ K. T. Flood,⁷⁷ Y. Pan,⁷⁷ R. Prepost,⁷⁷ C. O. Vuosalo,⁷⁷ and S. L. Wu⁷⁷

(The BABAR Collaboration)

¹Laboratoire d'Annecy-le-Vieux de Physique des Particules (LAPP),
Université de Savoie, CNRS/IN2P3, F-74941 Annecy-Le-Vieux, France

²Universitat de Barcelona, Facultat de Física, Departament ECM, E-08028 Barcelona, Spain

³INFN Sezione di Bari^a; Dipartimento di Fisica, Università di Bari^b, I-70126 Bari, Italy

⁴University of Bergen, Institute of Physics, N-5007 Bergen, Norway

⁵Lawrence Berkeley National Laboratory and University of California, Berkeley, California 94720, USA

⁶University of Birmingham, Birmingham, B15 2TT, United Kingdom

⁷Ruhr Universität Bochum, Institut für Experimentalphysik 1, D-44780 Bochum, Germany

⁸University of British Columbia, Vancouver, British Columbia, Canada V6T 1Z1

⁹Brunel University, Uxbridge, Middlesex UB8 3PH, United Kingdom

¹⁰Budker Institute of Nuclear Physics, Novosibirsk 630090, Russia

¹¹University of California at Irvine, Irvine, California 92697, USA

¹²University of California at Riverside, Riverside, California 92521, USA

¹³University of California at Santa Barbara, Santa Barbara, California 93106, USA

¹⁴University of California at Santa Cruz, Institute for Particle Physics, Santa Cruz, California 95064, USA

¹⁵California Institute of Technology, Pasadena, California 91125, USA

¹⁶University of Cincinnati, Cincinnati, Ohio 45221, USA

¹⁷University of Colorado, Boulder, Colorado 80309, USA

¹⁸Colorado State University, Fort Collins, Colorado 80523, USA

¹⁹Technische Universität Dortmund, Fakultät Physik, D-44221 Dortmund, Germany

²⁰Technische Universität Dresden, Institut für Kern- und Teilchenphysik, D-01062 Dresden, Germany

²¹Laboratoire Leprince-Ringuet, CNRS/IN2P3, Ecole Polytechnique, F-91128 Palaiseau, France

²²University of Edinburgh, Edinburgh EH9 3JZ, United Kingdom

²³INFN Sezione di Ferrara^a; Dipartimento di Fisica, Università di Ferrara^b, I-44100 Ferrara, Italy

²⁴INFN Laboratori Nazionali di Frascati, I-00044 Frascati, Italy

²⁵INFN Sezione di Genova^a; Dipartimento di Fisica, Università di Genova^b, I-16146 Genova, Italy

²⁶Indian Institute of Technology Guwahati, Guwahati, Assam, 781 039, India

²⁷Harvard University, Cambridge, Massachusetts 02138, USA

²⁸Universität Heidelberg, Physikalisches Institut, Philosophenweg 12, D-69120 Heidelberg, Germany

²⁹Humboldt-Universität zu Berlin, Institut für Physik, Newtonstr. 15, D-12489 Berlin, Germany

³⁰Imperial College London, London, SW7 2AZ, United Kingdom

³¹University of Iowa, Iowa City, Iowa 52242, USA

³²Iowa State University, Ames, Iowa 50011-3160, USA

³³Johns Hopkins University, Baltimore, Maryland 21218, USA

³⁴Laboratoire de l'Accélérateur Linéaire, IN2P3/CNRS et Université Paris-Sud 11,
Centre Scientifique d'Orsay, B. P. 34, F-91898 Orsay Cedex, France

³⁵Lawrence Livermore National Laboratory, Livermore, California 94550, USA

³⁶University of Liverpool, Liverpool L69 7ZE, United Kingdom

³⁷Queen Mary, University of London, London, E1 4NS, United Kingdom

³⁸University of London, Royal Holloway and Bedford New College, Egham, Surrey TW20 0EX, United Kingdom

³⁹University of Louisville, Louisville, Kentucky 40292, USA

- ⁴⁰Johannes Gutenberg-Universität Mainz, Institut für Kernphysik, D-55099 Mainz, Germany
⁴¹University of Manchester, Manchester M13 9PL, United Kingdom
⁴²University of Maryland, College Park, Maryland 20742, USA
⁴³University of Massachusetts, Amherst, Massachusetts 01003, USA
⁴⁴Massachusetts Institute of Technology, Laboratory for Nuclear Science, Cambridge, Massachusetts 02139, USA
⁴⁵McGill University, Montréal, Québec, Canada H3A 2T8
⁴⁶INFN Sezione di Milano^a; Dipartimento di Fisica, Università di Milano^b, I-20133 Milano, Italy
⁴⁷University of Mississippi, University, Mississippi 38677, USA
⁴⁸Université de Montréal, Physique des Particules, Montréal, Québec, Canada H3C 3J7
⁴⁹INFN Sezione di Napoli^a; Dipartimento di Scienze Fisiche, Università di Napoli Federico II^b, I-80126 Napoli, Italy
⁵⁰NIKHEF, National Institute for Nuclear Physics and High Energy Physics, NL-1009 DB Amsterdam, The Netherlands
⁵¹University of Notre Dame, Notre Dame, Indiana 46556, USA
⁵²Ohio State University, Columbus, Ohio 43210, USA
⁵³University of Oregon, Eugene, Oregon 97403, USA
⁵⁴INFN Sezione di Padova^a; Dipartimento di Fisica, Università di Padova^b, I-35131 Padova, Italy
⁵⁵Laboratoire de Physique Nucléaire et de Hautes Energies, IN2P3/CNRS, Université Pierre et Marie Curie-Paris6, Université Denis Diderot-Paris7, F-75252 Paris, France
⁵⁶INFN Sezione di Perugia^a; Dipartimento di Fisica, Università di Perugia^b, I-06100 Perugia, Italy
⁵⁷INFN Sezione di Pisa^a; Dipartimento di Fisica, Università di Pisa^b; Scuola Normale Superiore di Pisa^c, I-56127 Pisa, Italy
⁵⁸Princeton University, Princeton, New Jersey 08544, USA
⁵⁹INFN Sezione di Roma^a; Dipartimento di Fisica, Università di Roma La Sapienza^b, I-00185 Roma, Italy
⁶⁰Universität Rostock, D-18051 Rostock, Germany
⁶¹Rutherford Appleton Laboratory, Chilton, Didcot, Oxon, OX11 0QX, United Kingdom
⁶²CEA, Irfu, SPP, Centre de Saclay, F-91191 Gif-sur-Yvette, France
⁶³SLAC National Accelerator Laboratory, Stanford, California 94309 USA
⁶⁴University of South Carolina, Columbia, South Carolina 29208, USA
⁶⁵Southern Methodist University, Dallas, Texas 75275, USA
⁶⁶Stanford University, Stanford, California 94305-4060, USA
⁶⁷State University of New York, Albany, New York 12222, USA
⁶⁸Tel Aviv University, School of Physics and Astronomy, Tel Aviv, 69978, Israel
⁶⁹University of Tennessee, Knoxville, Tennessee 37996, USA
⁷⁰University of Texas at Austin, Austin, Texas 78712, USA
⁷¹University of Texas at Dallas, Richardson, Texas 75083, USA
⁷²INFN Sezione di Torino^a; Dipartimento di Fisica Sperimentale, Università di Torino^b, I-10125 Torino, Italy
⁷³INFN Sezione di Trieste^a; Dipartimento di Fisica, Università di Trieste^b, I-34127 Trieste, Italy
⁷⁴IFIC, Universitat de Valencia-CSIC, E-46071 Valencia, Spain
⁷⁵University of Victoria, Victoria, British Columbia, Canada V8W 3P6
⁷⁶Department of Physics, University of Warwick, Coventry CV4 7AL, United Kingdom
⁷⁷University of Wisconsin, Madison, Wisconsin 53706, USA

(Dated: August 31, 2018)

We study the processes $\gamma\gamma \rightarrow K_S^0 K^\pm \pi^\mp$ and $\gamma\gamma \rightarrow K^+ K^- \pi^+ \pi^- \pi^0$ using a data sample of 519.2 fb^{-1} recorded by the BABAR detector at the PEP-II asymmetric-energy e^+e^- collider at center-of-mass energies near the $\Upsilon(nS)$ ($n = 2, 3, 4$) resonances. We observe the $\eta_c(1S)$, $\chi_{c0}(1P)$ and $\eta_c(2S)$ resonances produced in two-photon interactions and decaying to $K^+ K^- \pi^+ \pi^- \pi^0$, with significances of 18.1, 5.4 and 5.3 standard deviations (including systematic errors), respectively, and report 4.0σ evidence of the $\chi_{c2}(1P)$ decay to this final state. We measure the $\eta_c(2S)$ mass and width in $K_S^0 K^\pm \pi^\mp$ decays, and obtain the values $m(\eta_c(2S)) = 3638.5 \pm 1.5 \pm 0.8 \text{ MeV}/c^2$ and $\Gamma(\eta_c(2S)) = 13.4 \pm 4.6 \pm 3.2 \text{ MeV}$, where the first uncertainty is statistical and the second is systematic. We measure the two-photon width times branching fraction for the reported resonance signals, and search for the $\chi_{c2}(2P)$ resonance, but no significant signal is observed.

PACS numbers: 13.25.Gv, 14.40.Pq

The first radial excitation $\eta_c(2S)$ of the $\eta_c(1S)$ charmonium ground state was observed at B -factories [1–4]. The only observed exclusive decay of this state to date is to $K\bar{K}\pi$ [5]. Decays to $p\bar{p}$ and $h^+h^-h'^+h'^-$, with $h^{(\prime)} = K, \pi$, have been observed for the $\eta_c(1S)$ [5], but

not for the $\eta_c(2S)$ [6, 7]. Precise determination of the $\eta_c(2S)$ mass may discriminate among models that predict the $\psi(2S)$ - $\eta_c(2S)$ mass splitting [8].

After the discovery of the $X(3872)$ state [9] and its confirmation by different experiments [10], charmonium

spectroscopy above the open-charm threshold received renewed attention. Many new states have been established to date [11–13]. The $Z(3930)$ resonance was discovered by Belle in the $\gamma\gamma\rightarrow D\bar{D}$ process [12] and subsequently confirmed by *BABAR* [13]. Its interpretation as the $\chi_{c2}(2P)$, the first radial excitation of the 3P_2 charmonium ground state, is commonly accepted [5].

In this paper we study charmonium resonances produced in the two-photon process $e^+e^-\rightarrow\gamma\gamma e^+e^-\rightarrow f e^+e^-$, where f denotes the $K_S^0 K^\pm \pi^\mp$ or $K^+ K^- \pi^+ \pi^- \pi^0$ final state. Two-photon events where the interacting photons are not quasi-real are strongly suppressed by the selection criteria described below. This implies that the allowed J^{PC} values of the initial state are $0^{\pm+}$, $2^{\pm+}$, $4^{\pm+}$, ...; 3^{++} , 5^{++} , ... [16]. Angular momentum conservation, parity conservation, and charge conjugation invariance, then imply that these quantum numbers apply to the final states f also, except that the $K_S^0 K^\pm \pi^\mp$ state cannot have $J^P = 0^+$.

The results presented here are based on data collected with the *BABAR* detector at the PEP-II asymmetric-energy e^+e^- collider, corresponding to an integrated luminosity of 519.2 fb^{-1} , recorded at center-of-mass (CM) energies near the $\Upsilon(nS)$ ($n = 2, 3, 4$) resonances.

The *BABAR* detector is described in detail elsewhere [14]. Charged-particles resulting from the interaction are detected, and their momenta are measured, by a combination of five layers of double-sided silicon microstrip detectors and a 40-layer drift chamber. Both systems operate in the 1.5 T magnetic field of a superconducting solenoid. Photons and electrons are identified in a CsI(Tl) crystal electromagnetic calorimeter. Charged-particle identification (PID) is provided by the specific energy loss (dE/dx) in the tracking devices, and by an internally reflecting, ring-imaging Cherenkov detector. Samples of Monte Carlo (MC) simulated events [15], which are more than 10 times larger than the corresponding data samples, are used to study signals and backgrounds. Two-photon events are generated using the GamGam generator [13].

Neutral pions and kaons are reconstructed through the decays $\pi^0\rightarrow\gamma\gamma$ and $K_S^0\rightarrow\pi^+\pi^-$. Photons from π^0 decays are required to have laboratory energy larger than 30 MeV. We require the invariant mass of a π^0 (K_S^0) candidate to be in the range [100–160] ([470–520]) MeV/c^2 . Neutral pions reconstructed with these criteria are used to veto events with multiple π^0 mesons, as described below. For the $K^+K^-\pi^+\pi^-\pi^0$ mode, we refine the selection of the π^0 by requiring the laboratory energy of the lower-energy photon from the signal π^0 decay to be larger than 50 MeV. Furthermore, we require $|\cos\mathcal{H}_{\pi^0}| < 0.95$, where \mathcal{H}_{π^0} is the angle between the signal π^0 flight direction in the laboratory frame and the direction of one of its daughters in the π^0 rest frame. These requirements are optimized by maximizing $S/\sqrt{S+B}$, where S is the number of MC signal events with a well-reconstructed

π^0 , and B is the combinatorial background in the signal region. Primary charged-particle tracks are required to satisfy PID requirements consistent with a kaon or pion hypothesis. A candidate event is constructed by fitting the π^0 (K_S^0) candidate and four (two) charged-particle tracks of zero net charge coming from the interaction region to a common vertex. In this fit the π^0 and K_S^0 masses are constrained to their nominal values [5]. We require the vertex fit probability of the charmonium candidate to be larger than 0.1%. The outgoing e^\pm are not detected.

Background arises mainly from random combinations of particles from e^+e^- annihilation, other two-photon collisions, and initial state radiation (ISR) processes. To suppress these backgrounds, we require that each event have exactly four charged-particle tracks. The candidate event is rejected if the number of additional reconstructed photons is larger than 6 (5) for $K^+K^-\pi^+\pi^-\pi^0$ ($K_S^0 K^\pm \pi^\mp$). Similarly, the event is rejected if the number of additional reconstructed π^0 's is larger than 1 (3) for a $K^+K^-\pi^+\pi^-\pi^0$ ($K_S^0 K^\pm \pi^\mp$) candidate event. We discriminate against ISR background by requiring $M_{\text{miss}}^2 = (p_{e^+e^-} - p_{\text{rec}})^2 > 2 (\text{GeV}/c^2)^2$, where $p_{e^+e^-}$ (p_{rec}) is the four momentum of the initial state (reconstructed final state). The effect of this requirement on the signal efficiency is studied using a $K^+K^-\pi^+\pi^-$ control sample that contains large $\eta_c(1S)$, J/ψ , and $\chi_{c0,2}(1P)$ signals. Two-photon events are expected to have low transverse momentum (p_T) with respect to the collision axis. In Fig. 1, we show the p_T distribution for selected candidates with the above requirements. The distribution is fitted with the signal p_T shape obtained from MC simulation plus a combinatorial background component, modeled using a sixth-order polynomial function. We require $p_T < 0.15 \text{ GeV}/c$.

The average number of surviving candidates per selected event is 1.003 (1.09) for the $K_S^0 K^\pm \pi^\mp$ ($K^+K^-\pi^+\pi^-\pi^0$) final state. Candidates that are rejected by a possible best-candidate selection do not lead to any peaking structures in the mass spectra, and so no best-candidate selection is performed. The $K_S^0 K^+ \pi^-$ and $K^+K^-\pi^+\pi^-\pi^0$ mass spectra are shown in Fig. 2. We observe prominent peaks at the position of the $\eta_c(1S)$ resonance. We also observe signals at the positions of the J/ψ , $\chi_{c0}(1P)$, $\chi_{c2}(1P)$, and $\eta_c(2S)$ states.

The resonance signal yields and the mass and width of the $\eta_c(1S)$ and $\eta_c(2S)$ are extracted using a binned, extended maximum likelihood fit to the invariant mass distributions. The bin width is $4 \text{ MeV}/c^2$. In the likelihood function, several components are present: $\eta_c(1S)$, $\chi_{c0}(1P)$, $\chi_{c2}(1P)$, and $\eta_c(2S)$ signal, combinatorial background, and J/ψ ISR background. The $\chi_{c0}(1P)$ component is not present in the fit to the $K_S^0 K^\pm \pi^\mp$ invariant mass spectrum, since $J^P = 0^+$ is forbidden for this final state.

We parameterize each signal PDF as a convolution of

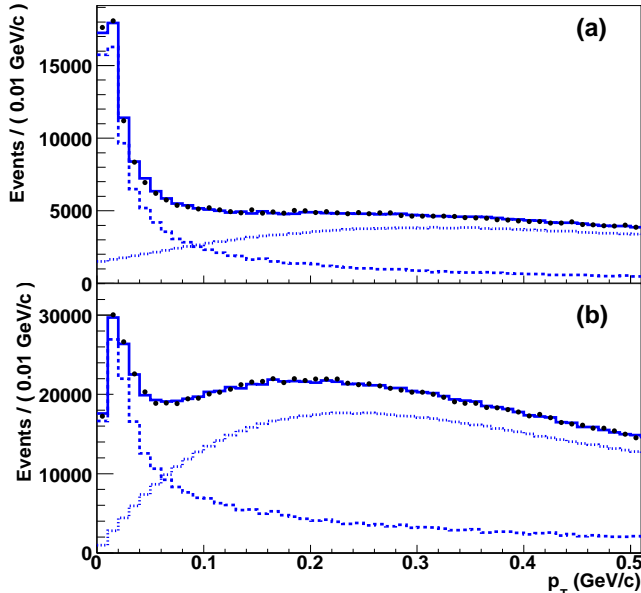


FIG. 1: The p_T distributions for selected (a) $K_S^0 K^\pm \pi^\mp$ and (b) $K^+ K^- \pi^+ \pi^- \pi^0$ candidates (data points). The solid histogram represent the result of a fit to the sum of the simulated signal (dashed) and background (dotted) contributions.

a non-relativistic Breit-Wigner and the detector resolution function. The J/ψ ISR background is parameterized with a Gaussian shape, and the combinatorial background PDF is a fourth-order polynomial. The free parameters of the fit are the yields of the resonances and the background, the peak masses and widths of the $\eta_c(1S)$ and $\eta_c(2S)$ signals, the width of the Gaussian describing the J/ψ ISR background, and the background shape parameters. The mass and width of the $\chi_{c0,2}(1P)$ states (and the mass of the J/ψ in the $K_S^0 K^\pm \pi^\mp$ channel), are fixed to their nominal values [5]. For the $K^+ K^- \pi^+ \pi^- \pi^0$ channel, the $\eta_c(2S)$ width is fixed to the value found in the $K_S^0 K^\pm \pi^\mp$ channel.

We define a MC event as ‘‘MC-Truth’’ (MCT) if the reconstructed decay chain matches the generated one. We use MCT signal and MCT ISR-background events to determine the detector mass resolution function. This function is described by the sum of a Gaussian plus power-law tails [17]. The width of the resolution function at half-maximum for the $\eta_c(1S)$ is 8.1 (11.8) MeV/c^2 in the $K_S^0 K^\pm \pi^\mp$ ($K^+ K^- \pi^+ \pi^- \pi^0$) decay mode. For the $\eta_c(2S)$ decay it is 10.6 (13.1) MeV/c^2 in the $K_S^0 K^\pm \pi^\mp$ ($K^+ K^- \pi^+ \pi^- \pi^0$) decay mode. The parameter values for the resolution functions, are fixed to their MC values in the fit.

Fit results are reported in Table I and shown in Fig. 2. We correct the fitted $\eta_c(1S)$ yields by subtracting the number of peaking-background events originating from

the $J/\psi \rightarrow \gamma \eta_c(1S)$ decay, estimated below. The statistical significances of the signal yields are computed from the ratio of the number of observed events to the sum in quadrature of the statistical and systematic uncertainties. The χ^2/ndf of the fit is 1.07 (1.03), where ndf is the number of degrees of freedom, which is 361 (360) for the fit to $K_S^0 K^\pm \pi^\mp$ ($K^+ K^- \pi^+ \pi^- \pi^0$).

To search for the $\chi_{c2}(2P)$, we add to the fit described above a signal component with the mass and width fixed to the values reported in Ref. [13]. No significant changes are observed in the fit results. Several processes, includ-

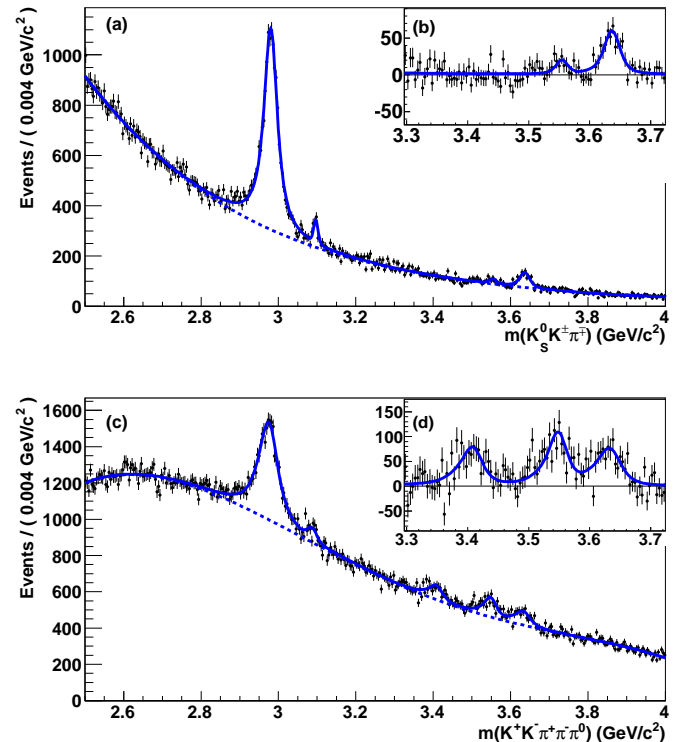


FIG. 2: Fit to (a) the $K_S^0 K^\pm \pi^\mp$ and (c) the $K^+ K^- \pi^+ \pi^- \pi^0$ mass spectrum. The solid curves represent the total fit functions and the dashed curves show the combinatorial background contributions. The background-subtracted distributions are shown in (b) and (d), where the solid curves indicate the signal components.

ing ISR, continuum e^+e^- annihilation, and two-photon events with a final state different from the one studied, may produce irreducible-peaking-background events, containing real $\eta_c(1S)$, $\eta_c(2S)$, $\chi_{c0}(1P)$ or $\chi_{c2}(1P)$. Well-reconstructed signal and J/ψ ISR background are expected to peak at $p_T \sim 0$ GeV/c . Final states with similar masses are expected to have similar p_T distributions. Non-ISR background events mainly originate from events with a number of particles in the final state larger than the one in signal events. Such extra particles are lost in the reconstruction. Thus, non-ISR background

TABLE I: Extraction of event yields and mass and width of the $\eta_c(1S)$ and $\eta_c(2S)$ resonances: average signal efficiency for phase-space MCT events, corrected signal yield with statistical and systematic uncertainties, number of peaking-background events estimated with the p_T fit (N_{peak}), number of peaking-background events from J/ψ and $\psi(2S)$ radiative decays (N_ψ), significance (including systematic uncertainty), corrected mass, and fitted width for each decay mode. We do not report N_ψ for modes where it is negligible.

Decay Mode	Efficiency (%)	Corrected Yield (Evs.)	N_{peak} (Evs.)	N_ψ (Evs.)	Significance (σ)	Corrected Mass (MeV/ c^2)	Fitted Width (MeV)
$\eta_c(1S) \rightarrow K_s^0 K^\pm \pi^\mp$	10.7	$12096 \pm 235 \pm 274$	189 ± 18	214 ± 82	33.5	$2982.5 \pm 0.4 \pm 1.4$	$32.1 \pm 1.1 \pm 1.3$
$\chi_{c2}(1P) \rightarrow K_s^0 K^\pm \pi^\mp$	13.1	$126 \pm 37 \pm 14$	-45 ± 11	–	3.2	3556.2 (fixed)	2 (fixed)
$\eta_c(2S) \rightarrow K_s^0 K^\pm \pi^\mp$	13.3	$624 \pm 72 \pm 34$	25 ± 5	–	7.8	$3638.5 \pm 1.5 \pm 0.8$	$13.4 \pm 4.6 \pm 3.2$
$\eta_c(1S) \rightarrow K^+ K^- \pi^+ \pi^- \pi^0$	4.2	$11132 \pm 430 \pm 442$	118 ± 32	26 ± 9	18.1	$2984.5 \pm 0.8 \pm 3.1$	$36.2 \pm 2.8 \pm 3.0$
$\chi_{c0}(1P) \rightarrow K^+ K^- \pi^+ \pi^- \pi^0$	5.6	$1094 \pm 143 \pm 143$	-39 ± 19	75 ± 21	5.4	3415.8 (fixed)	10.2 (fixed)
$\chi_{c2}(1P) \rightarrow K^+ K^- \pi^+ \pi^- \pi^0$	5.8	$1250 \pm 118 \pm 290$	14 ± 24	233 ± 73	4.0	3556.2 (fixed)	2 (fixed)
$\eta_c(2S) \rightarrow K^+ K^- \pi^+ \pi^- \pi^0$	5.9	$1201 \pm 133 \pm 185$	-46 ± 17	–	5.3	$3640.5 \pm 3.2 \pm 2.5$	13.4 (fixed)

events are expected to have a nearly flat p_T distribution, as observed in MC simulation.

To estimate the number of such events, we fit the invariant mass distribution in intervals of p_T , thus obtaining the signal yield for each resonance as a function of p_T . The signal yield distribution is then fitted using the signal p_T shape from MCT events plus a flat background. The yield of peaking-background events originating from ψ radiative decays ($\psi = J/\psi, \psi(2S)$) is estimated using the number of ψ events fitted in data, and the knowledge of branching fractions [5] and MC reconstruction efficiencies for the different decays involved. The number of peaking-background events for each resonance is reported in Table I. The value of $\mathcal{B}(\chi_{c0,2} \rightarrow K^+ K^- \pi^+ \pi^- \pi^0)$, which is needed to estimate the number of peaking-background events from $\psi(2S) \rightarrow \gamma \chi_{c0,2}(1P)$ decays, is obtained using the results reported in this paper and the world-average values of $\Gamma_{\gamma\gamma}(\chi_{c0,2})$ [5]. We obtain $\mathcal{B}(\chi_{c0}(1P) \rightarrow K^+ K^- \pi^+ \pi^- \pi^0) = (1.14 \pm 0.27)\%$, and $\mathcal{B}(\chi_{c2}(1P) \rightarrow K^+ K^- \pi^+ \pi^- \pi^0) = (1.30 \pm 0.36)\%$, where statistical and systematic errors have been summed in quadrature. The value of $\mathcal{B}(\chi_{c2}(1P) \rightarrow K^+ K^- \pi^+ \pi^- \pi^0)$ is in agreement with a preliminary result reported by CLEO [18]. The number of peaking background events from ψ radiative decays for $\eta_c(2S)$ and $\chi_{c2}(1P) \rightarrow K_s^0 K^\pm \pi^\mp$ (denoted by “–” in Table I) is negligible.

The ratios of the branching fractions of the two modes are obtained from

$$\frac{\mathcal{B}(\eta_c(nS) \rightarrow K^+ K^- \pi^+ \pi^- \pi^0)}{\mathcal{B}(\eta_c(nS) \rightarrow K_s^0 K^\pm \pi^\mp)} = \frac{N_{KK3\pi}^{\eta_c(nS)}}{N_{K_s^0 K\pi}^{\eta_c(nS)}} \cdot \frac{\epsilon_{K_s^0 K\pi}^{\eta_c(nS)}}{\epsilon_{KK3\pi}^{\eta_c(nS)}}, \quad (1)$$

where $\eta_c(nS)$ denotes $\eta_c(1S)$, $\eta_c(2S)$; $N_{KK3\pi}^{\eta_c(nS)}$ and $N_{K_s^0 K\pi}^{\eta_c(nS)}$ ($\epsilon_{KK3\pi}^{\eta_c(nS)}$ and $\epsilon_{K_s^0 K\pi}^{\eta_c(nS)}$) represent the peaking-background-subtracted $\eta_c(nS)$ yield (the efficiency) for the $K^+ K^- \pi^+ \pi^- \pi^0$ and $K_s^0 K^\pm \pi^\mp$ channels, respectively. The efficiencies are parameterized using MCT events. The $K_s^0 K^\pm \pi^\mp$ efficiency is parameterized as a two-dimensional histogram of the invariant $K\pi$ mass versus

the angle between the direction of the K^+ in the $K\pi$ rest frame and that of the $K\pi$ system in the $K_s^0 K^\pm \pi^\mp$ reference frame. The $K^+ K^- \pi^+ \pi^- \pi^0$ efficiency is parameterized as a function of the $K^+ K^-$, $\pi^+ \pi^-$, and $\pi^+ \pi^- \pi^0$ (3π) masses, and the five angular variables, $\cos \theta_K$, $\cos \Theta$, Φ , $\cos \theta_{\pi\pi}$, and θ_π , as defined in Fig. 3; θ_K is the angle

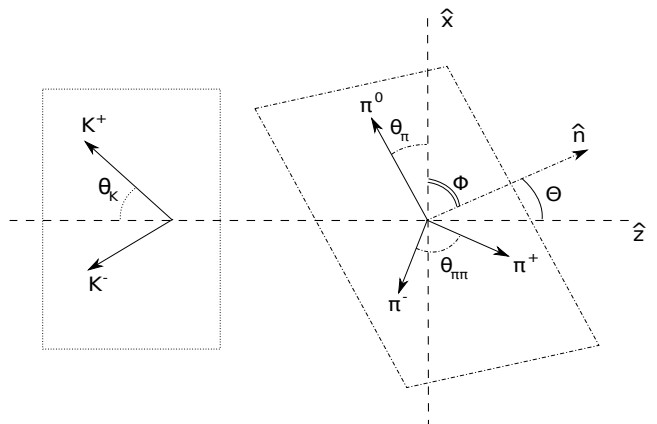


FIG. 3: Angles used to describe the $K^+ K^- \pi^+ \pi^- \pi^0$ decay kinematics

between the K^+ and the 3π recoil direction in the $K^+ K^-$ rest frame. The angles Θ and Φ describe the orientation of the normal \hat{n} to the 3π decay plane with respect to the $K^+ K^-$ recoil direction in the 3π rest frame; θ_π is the angle describing a rotation of the 3π system about its decay plane normal; $\theta_{\pi\pi}$ is the angle between the π^+ and π^- directions in the 3π reference frame. The correlations between $\cos \theta_K$, Θ , Φ , and θ_π and the invariant masses are negligible. The correlation between $\cos \theta_{\pi\pi}$ and $m_{\pi\pi}$ is -0.70 and is not considered in the efficiency parameterization. Neglecting such a correlation introduces a change in the efficiency of 1.4% (1.1%) for the $\eta_c(1S)$ ($\eta_c(2S)$), which is taken as a systematic uncertainty. The efficiency dependence on $\cos \theta_K$, $\cos \theta_{\pi\pi}$, and Φ ($\cos \Theta$ and θ_π) is parameterized using uncorrelated fourth(second)-order polynomial shapes. A three-dimensional histogram

is used to parameterize the dependence on the invariant masses. The efficiency is calculated as the ratio of the number of MCT events surviving the selection to the number of generated events in each bin, in both channels. We assign null efficiency to bins with less than 10 reconstructed events. The fraction of data falling in these bins is 0.5% (3.0%) in the $K_s^0 K^\pm \pi^\mp$ ($K^+ K^- \pi^+ \pi^- \pi^0$) channel. We assign a systematic uncertainty to cover this effect. The average efficiency $\bar{\epsilon}$ for each decay, computed using flat phase-space simulation, is reported in Table I.

The ratio N_f^η/ϵ_f^η of Eq. (1) is equal to $N_f^\eta/(\epsilon_f^{*\eta} \times \bar{\epsilon}_f^\eta)$, where we have defined $\epsilon_f^{*\eta} = \epsilon_f^\eta/\bar{\epsilon}_f^\eta$. The value of $N_f^\eta/\epsilon_f^{*\eta}$ is extracted from an unbinned maximum likelihood fit to the $K_s^0 K^\pm \pi^\mp$ and $K^+ K^- \pi^+ \pi^- \pi^0$ invariant mass distributions, where each event is weighted by the inverse of $\epsilon_f^{*\eta}$. We use $\epsilon_f^{*\eta}$ instead of ϵ_f^η to weight the events since weights far from one might result in incorrect errors for the signal yield obtained in the maximum likelihood fit [19]. Since the kinematics of peaking-background events are similar to those of the signal, we assume the signal to peaking-background ratio to be unaffected by the weighting technique. The fit is performed independently in the $\eta_c(1S)$ ([2.5, 3.3] GeV/ c^2) and $\eta_c(2S)$ ([3.2, 3.9] GeV/ c^2) mass regions. The mass and width for each signal PDF are fixed to the values reported in Table I. The free parameters of the fit are the yields of the background and the signal resonances, the mean and the width of the Gaussian describing the J/ψ background, and the background shape parameters. We compute a χ^2 using the total fit function and the binned $K_s^0 K^\pm \pi^\mp$ ($K^+ K^- \pi^+ \pi^- \pi^0$) mass distribution obtained after weighting. The values of χ^2/ndf are 1.16 (1.15) and 1.20 (1.00) in the $\eta_c(1S)$ and $\eta_c(2S)$ mass regions, in the $K_s^0 K^\pm \pi^\mp$ ($K^+ K^- \pi^+ \pi^- \pi^0$) channel.

Several sources contribute to systematic uncertainties on the resonance yields and parameters. Systematic uncertainties due to PDF parameterization and fixed parameters in the fit are estimated to be the sum in quadrature of the changes observed when repeating the fit after varying the fixed parameters by ± 1 standard deviation (σ). The uncertainty associated with the peaking background is taken to be $\sqrt{(\max[0, N_{\text{peak}}])^2 + \sigma_{N_{\text{peak}}}^2}$, where N_{peak} is the estimated number of peaking-background events reported in Table I, and $\sigma_{N_{\text{peak}}}$ is its uncertainty. The systematic errors on the $\chi_{c0,2}(1P)$ yields are taken to be $\sqrt{(\max[0, N_{\text{peak}}])^2 + \sigma_{N_{\text{peak}}}^2 + N_\psi^2 + \sigma_{N_\psi}^2}$, where N_ψ is the number of peaking-background events from the $\psi(2S) \rightarrow \gamma \chi_{c0,2}(1P)$ processes. The uncertainty on N_{peak} due to differences in signal and ISR background p_T distribution is estimated by adding an ISR background component to the fit to the p_T yield distribution described above. The ISR background p_T shape is taken from MC simulation and its yield is fixed to N_ψ . This uncertainty is found to be negligible. We take the systematic error due to the $J/\psi \rightarrow \gamma \eta_c(1S)$ peaking-background subtrac-

tion to be the uncertainty on the estimated number of events originating from this process. We assign an uncertainty due to the background shape, taking the changes in results observed when using a sixth-order polynomial as the background PDF in the fit.

An ISR-enriched sample is obtained by reversing the M_{miss}^2 selection criterion. The ISR-enriched sample is fitted to obtain the shift ΔM between the measured and the nominal J/ψ mass [5], and the difference in mass resolution between MC and data. The corrected masses in Table I are $m^{\text{corr}} = m^{\text{fit}} - \Delta M$, where m^{fit} is the mass determined by the fit. The mass shift is -0.5 ± 0.2 MeV/ c^2 in $K_s^0 K^\pm \pi^\mp$ and -1.1 ± 0.8 MeV/ c^2 in $K^+ K^- \pi^+ \pi^- \pi^0$. We assign the statistical error on ΔM as a systematic uncertainty on m^{corr} . The difference in mass resolution is $(24 \pm 5)\%$ in $K_s^0 K^\pm \pi^\mp$ and $(9 \pm 5)\%$ in $K^+ K^- \pi^+ \pi^- \pi^0$. We take the difference in fit results observed when including this correction in the $\eta_c(1S)$, $\chi_{c0}(1P)$, $\chi_{c2}(1P)$, and $\eta_c(2S)$ resolution functions as the systematic uncertainty due to the mass-resolution difference between data and MC. A systematic uncertainty on the mass accounts for the different kinematics of two-photon signal and ISR J/ψ events.

The distortion of the resolution function due to differences between the invariant mass distributions of the decay products in data and MC produces negligible changes in the results. We take as systematic uncertainty the changes in the resonance parameters observed by including in the fit the effect of the efficiency dependence on the invariant mass and on the decay dynamics. The effect of the interference of the $\eta_c(1S)$ signal with a possible $J^{PC} = 0^{-+}$ contribution in the $\gamma\gamma$ background is considered. We model the mass distribution of the $J^{PC} = 0^{-+}$ background component with the PDF describing combinatorial background. The changes in the fitted signal yields are negligible. The changes of the values of the $\eta_c(1S)$ mass and width with respect to the nominal results are $+1.2$ MeV/ c^2 and $+0.2$ MeV for $K_s^0 K^\pm \pi^\mp$, and $+2.9$ MeV/ c^2 and $+0.6$ MeV for $K^+ K^- \pi^+ \pi^- \pi^0$. We take these changes as estimates of systematic uncertainty due to interference. The effect of the interference on the $\eta_c(2S)$ parameter values cannot be determined due to the small signal to background ratio and the smallness of the signal sample. We therefore do not include any systematic uncertainty due to this effect for the $\eta_c(2S)$.

Systematic uncertainties on the efficiency due to tracking (0.2% per track), K_s^0 reconstruction (1.7%), π^0 reconstruction (3.0%) and PID (0.5% per track) are obtained from auxiliary studies. The statistical uncertainty of the efficiency parameterization is estimated with simulated parameterized experiments. In each experiment, the efficiency in each histogram bin and the coefficients of the functions describing the dependence on $\cos\theta_K$, $\cos\theta_{\pi\pi}$, $\cos\Theta$, θ_π and Φ are varied within their statistical uncertainties. We take as systematic uncertainty the width of the resulting yield distribution. The fit bias is negli-

ble. The small impact of the presence of events falling in bins with zero efficiency is accounted for as an additional systematic uncertainty.

Using the efficiency-weighted yields of the $\eta_c(1S)$ and $\eta_c(2S)$ resonances, the number of peaking-background events, and $\mathcal{B}(K_s^0 \rightarrow \pi^+ \pi^-) = (69.20 \pm 0.05)\%$ [5], we find the branching fraction ratios

$$\frac{\mathcal{B}(\eta_c(1S) \rightarrow K^+ K^- \pi^+ \pi^- \pi^0)}{\mathcal{B}(\eta_c(1S) \rightarrow K_s^0 K^\pm \pi^\mp)} = 1.43 \pm 0.05 \pm 0.21, \quad (2)$$

$$\frac{\mathcal{B}(\eta_c(2S) \rightarrow K^+ K^- \pi^+ \pi^- \pi^0)}{\mathcal{B}(\eta_c(2S) \rightarrow K_s^0 K^\pm \pi^\mp)} = 2.2 \pm 0.5 \pm 0.5, \quad (3)$$

where the first error is statistical and the second is systematic. The uncertainty in the efficiency parameterization is the main contribution to the systematic uncertainties and is equal to 0.17 and 0.3, in Eqs. (2) and (3), respectively. Using Eqs. (2)–(3), $\mathcal{B}(\eta_c(1S) \rightarrow K \bar{K} \pi) = (7.0 \pm 1.2)\%$ and $\mathcal{B}(\eta_c(2S) \rightarrow K \bar{K} \pi) = (1.9 \pm 1.2)\%$ [5], and isospin relations, we obtain $\mathcal{B}(\eta_c(1S) \rightarrow K^+ K^- \pi^+ \pi^- \pi^0) = (3.3 \pm 0.8)\%$, and $\mathcal{B}(\eta_c(2S) \rightarrow K^+ K^- \pi^+ \pi^- \pi^0) = (1.4 \pm 1.0)\%$, where we have summed in quadrature the statistical and systematic errors.

For each resonance and each final state, we compute the product between the two-photon coupling $\Gamma_{\gamma\gamma}$ and the resonance branching fraction \mathcal{B} to the final state, using 473.8 fb^{-1} of data collected near the $\Upsilon(4S)$ energy. The efficiency-weighted yields for the resonances, and the integrated luminosity near the $\Upsilon(4S)$ energy are used to obtain $\Gamma_{\gamma\gamma} \times \mathcal{B}$ with the GamGam generator [13]. The mass and width of the resonances are fixed to the values reported in Table I. The uncertainties on the luminosity (1.1%) and on the GamGam calculation (3%) [13] are included in the systematic uncertainty of $\Gamma_{\gamma\gamma} \times \mathcal{B}$. For the $K_s^0 K^\pm \pi^\mp$ decay mode, we give the results for the isospin-related $K \bar{K} \pi$ final state, taking into account $\mathcal{B}(K_s^0 \rightarrow \pi^+ \pi^-) = (69.20 \pm 0.05)\%$ [5] and isospin relations. For the $\chi_{c2}(2P)$, we compute $\Gamma_{\gamma\gamma} \times \mathcal{B}$ using the fitted $\chi_{c2}(2P)$ yield, the integrated luminosity near the $\Upsilon(4S)$ energy, and the average detection efficiency for the relevant process. The average detection efficiency is equal to 13.9% and 6.4% for the $K_s^0 K^\pm \pi^\mp$ and $K^+ K^- \pi^+ \pi^- \pi^0$ modes, respectively. The mass and width of the $\chi_{c2}(2P)$ resonance are fixed to the values reported in [13]. Since no significant $\chi_{c2}(2P)$ signal is observed, we determine a Bayesian upper limit (UL) at 90% confidence level (CL) on $\Gamma_{\gamma\gamma} \times \mathcal{B}$, assuming a uniform prior probability distribution. We compute the UL by finding the value of $\Gamma_{\gamma\gamma} \times \mathcal{B}$ below which lies 90% of the total of the likelihood integral in the $(\Gamma_{\gamma\gamma} \times \mathcal{B}) \geq 0$ region. Systematic uncertainties are taken into account in the UL calculation. Results for $\Gamma_{\gamma\gamma} \times \mathcal{B}$ for each resonance and final state are reported in Table II. The $\eta_c(1S) \rightarrow K \bar{K} \pi$ measurement is consistent with, but slightly more precise than, the PDG value [5]; the other entries are first measurements.

TABLE II: Results for $\Gamma_{\gamma\gamma} \times \mathcal{B}$ for each resonance in $K \bar{K} \pi$ and $K^+ K^- \pi^+ \pi^- \pi^0$ final states. The first uncertainty is statistical, the second systematic. Upper limits are computed at 90% confidence level.

Process	$\Gamma_{\gamma\gamma} \times \mathcal{B}$ (keV)
$\eta_c(1S) \rightarrow K \bar{K} \pi$	$0.386 \pm 0.008 \pm 0.021$
$\chi_{c2}(1P) \rightarrow K \bar{K} \pi$	$(1.8 \pm 0.5 \pm 0.2) \times 10^{-3}$
$\eta_c(2S) \rightarrow K \bar{K} \pi$	$0.041 \pm 0.004 \pm 0.006$
$\chi_{c2}(2P) \rightarrow K \bar{K} \pi$	$< 2.1 \times 10^{-3}$
$\eta_c(1S) \rightarrow K^+ K^- \pi^+ \pi^- \pi^0$	$0.190 \pm 0.006 \pm 0.028$
$\chi_{c0}(1P) \rightarrow K^+ K^- \pi^+ \pi^- \pi^0$	$0.026 \pm 0.004 \pm 0.004$
$\chi_{c2}(1P) \rightarrow K^+ K^- \pi^+ \pi^- \pi^0$	$(6.5 \pm 0.9 \pm 1.5) \times 10^{-3}$
$\eta_c(2S) \rightarrow K^+ K^- \pi^+ \pi^- \pi^0$	$0.030 \pm 0.006 \pm 0.005$
$\chi_{c2}(2P) \rightarrow K^+ K^- \pi^+ \pi^- \pi^0$	$< 3.4 \times 10^{-3}$

In conclusion, we report the first observation of $\eta_c(1S)$, $\chi_{c0}(1P)$ and $\eta_c(2S)$ decays to $K^+ K^- \pi^+ \pi^- \pi^0$, with significances (including systematic uncertainties) of 18σ , 5.4σ and 5.3σ , respectively. This is the first observation of an exclusive hadronic decay of $\eta_c(2S)$ other than $K \bar{K} \pi$. We also report the first evidence of $\chi_{c2}(1P)$ decays to $K^+ K^- \pi^+ \pi^- \pi^0$, with a significance (including systematic uncertainties) of 4.0σ , and have obtained first measurements of the $\chi_{c0}(1P)$ and $\chi_{c2}(1P)$ branching fractions to $K^+ K^- \pi^+ \pi^- \pi^0$. The measurements reported in this paper are consistent with previous *BABAR* results [3, 20], and with world average values [5]. The measurement of the $\eta_c(2S)$ mass and width in the the $K_s^0 K^\pm \pi^\mp$ decay supersedes the previous *BABAR* measurement [3]. The measurement of the $\eta_c(1S)$ mass and width in the the $K_s^0 K^\pm \pi^\mp$ decay does not supersede the previous *BABAR* measurement [20]. The value of $\Gamma_{\gamma\gamma} \times \mathcal{B}$ is measured for each observed resonance for both $K \bar{K} \pi$ and $K^+ K^- \pi^+ \pi^- \pi^0$ decay modes. We provide an UL at 90% CL on $\Gamma_{\gamma\gamma} \times \mathcal{B}$ for the $\chi_{c2}(2P)$ resonance.

We thank C. P. Shen and M. Shepherd for useful discussions. We are grateful for the excellent luminosity and machine conditions provided by our PEP-II colleagues, and for the substantial dedicated effort from the computing organizations that support *BABAR*. The collaborating institutions wish to thank SLAC for its support and kind hospitality. This work is supported by DOE and NSF (USA), NSERC (Canada), CEA and CNRS-IN2P3 (France), BMBF and DFG (Germany), INFN (Italy), FOM (The Netherlands), NFR (Norway), MES (Russia), MICINN (Spain), STFC (United Kingdom). Individuals have received support from the Marie Curie EIF (European Union), the A. P. Sloan Foundation (USA) and the Binational Science Foundation (USA-Israel).

* Now at Temple University, Philadelphia, Pennsylvania 19122, USA

† Also with Università di Perugia, Dipartimento di Fisica,

Perugia, Italy

‡ Also with Università di Roma La Sapienza, I-00185 Roma, Italy

§ Now at University of South Alabama, Mobile, Alabama 36688, USA

¶ Also with Università di Sassari, Sassari, Italy

- [1] S. K Choi *et al.* (Belle Collaboration), Phys. Rev. Lett. **89**, 102001 (2002); K. Abe *et al.* (Belle Collaboration), Phys. Rev. Lett. **89**, 142001 (2002).
- [2] D. M. Asner *et al.* (CLEO Collaboration), Phys. Rev. Lett. **92**, 142001 (2004).
- [3] B. Aubert *et al.* (BABAR Collaboration), Phys. Rev. Lett. **92**, 142002 (2004).
- [4] B. Aubert *et al.* (BABAR Collaboration), Phys. Rev. Lett. **96**, 052002 (2006).
- [5] Particle Data Group, K. Nakamura *et al.*, J. Phys. G **37**, 075021 (2010).
- [6] S. Uehara *et al.* (Belle Collaboration), Eur. Phys. Jour. C **53**, 1 (2008).
- [7] M. Ambrogiani *et al.* (E835 Collaboration), Phys. Rev. D **64**, 052003 (2001).
- [8] S. Godfrey and N. Isgur, Phys. Rev. D **32**, 189 (1985); L. P. Fulcher, Phys. Rev. D **44**, 2079 (1991); J. Zeng *et al.*, Phys. Rev. D **52**, 5229 (1995); S. N. Gupta and J. M. Johnson, Phys. Rev. D **53**, 312 (1996); D. Ebert *et al.*, Phys. Rev. D **67**, 014027 (2003); E. Eichten *et al.*, Phys. Rev. D **69**, 094019 (2004).
- [9] S.-K. Choi *et al.* (Belle Collaboration), Phys. Rev. Lett. **91**, 262001 (2003).
- [10] D. E. Acosta *et al.* (CDF Collaboration), Phys. Rev. Lett. **93**, 072001 (2004); V. M. Abazov *et al.* (D0 Collaboration), Phys. Rev. Lett. **93**, 162002 (2004); B. Aubert *et al.* (BABAR Collaboration), Phys. Rev. D **71**, 071103 (2005).
- [11] B. Aubert *et al.* (BABAR Collaboration), Phys. Rev. Lett. **95**, 142001 (2005); T. E. Coan *et al.* (CLEO Collaboration), Phys. Rev. Lett. **96**, 162003 (2006); C. Z. Yuan *et al.* (Belle Collaboration), Phys. Rev. Lett. **99**, 182004 (2007); B. Aubert *et al.* (BABAR Collaboration), Phys. Rev. Lett. **98**, 212001 (2007); X. L. Wang *et al.* (Belle Collaboration), Phys. Rev. Lett. **99**, 142002 (2007); S.-K. Choi *et al.* (Belle Collaboration), Phys. Rev. Lett. **94**, 182002 (2005); B. Aubert *et al.* (BABAR Collaboration), Phys. Rev. Lett. **101**, 082001 (2008).
- [12] S. Uehara *et al.* (Belle Collaboration), Phys. Rev. Lett. **96**, 082003 (2006).
- [13] B. Aubert *et al.* (BABAR Collaboration), Phys. Rev. D **81**, 092003 (2010).
- [14] B. Aubert *et al.* (BABAR Collaboration), Nucl. Instrum. Methods Phys. Res., Sect. A **479**, 1 (2002).
- [15] The BABAR detector Monte Carlo simulation is based on GEANT4: S. Agostinelli *et al.*, Nucl. Instrum. Methods Phys. Res., Sect. A **506**, 250 (2003).
- [16] C. N. Yang, Phys. Rev. **77**, 242 (1950).
- [17] The power law tails are described by the function $B(x) = \frac{(\Gamma_{(1,2)}/2)^{\beta_{(1,2)}}}{|x-x_0|^{\beta_{(1,2)}} + (\Gamma_{(1,2)}/2)^{\beta_{(1,2)}}}$, where x_0 is a parameter, $\Gamma_1(\Gamma_2)$ and $\beta_1(\beta_2)$ are used when $x < x_0$ ($x > x_0$); see Ref. [20] for more information.
- [18] K. Gao, Ph.D. Thesis, University of Minnesota, 2008, arXiv:0909.2818[hep-ex]; B. Heltsley, “New CLEO Results on Charmonium Transitions”, The Sixth International Workshop on Heavy Quarkonia, Nara, Japan, 2008, http://www-conf.kek.jp/qwg08/session1_3/heltsley.pdf.
- [19] A. G. Frodesen *et al.*, *Probability and Statistics in Particle Physics* (Universitetsforlaget, Bergen, Norway, 1979).
- [20] J. P. Lees *et al.* (BABAR Collaboration), Phys. Rev. D **81**, 052010 (2010).